



Published in final edited form as:

*Nat Methods*. 2010 October ; 7(10): 821–824. doi:10.1038/nmeth.1508.

## Quantitative dynamic footprinting microscopy reveals mechanisms of neutrophil rolling

Prithu Sundd<sup>1</sup>, Edgar Gutierrez<sup>2</sup>, Maria K. Pospieszalska<sup>1</sup>, Hong Zhang<sup>1</sup>, Alexander Groisman<sup>2</sup>, and Klaus Ley<sup>1,\*</sup>

<sup>1</sup>Division of Inflammation Biology, La Jolla Institute for Allergy and Immunology, La Jolla, CA, 92037

<sup>2</sup>Department of Physics, University of California San Diego, La Jolla, CA, 92093

### Abstract

We introduce quantitative dynamic footprinting microscopy to resolve neutrophil rolling on P-selectin. We show that the footprint of a rolling neutrophil is four times larger than previously thought, the P-selectin-PSGL-1 bonds are relaxed at the leading edge of the rolling cell, compressed under the cell center, and stretched at the trailing edge. Each rolling neutrophil also forms 3-4 long tethers that extend up to 16  $\mu\text{m}$  behind the rolling cell.

Efficient neutrophil recruitment is essential for host defense and requires P-selectin-mediated rolling at high shear stress<sup>1</sup>. P-selectin is an adhesion molecule expressed on the surface of activated endothelial cells<sup>2</sup> at 20 to 50 molecules/ $\mu\text{m}^2$ . In microvessels *in vivo*<sup>3</sup> and in whole blood flow chambers *in vitro*<sup>4</sup>, neutrophils roll at wall shear stresses of 6 dyn/cm<sup>2</sup> and above. Numerical simulations with Adhesive Dynamics (AD<sup>5</sup>) or Event-Tracking (ETMA<sup>6</sup>) models of adhesion, using experimentally measured properties of the relevant adhesion molecules and cells, reproduce cell rolling at low shear stresses but fail to reproduce stable rolling at the higher shear stresses commonly observed *in vivo*. Thus, the mechanisms that allow neutrophils to roll at high shear stress remain elusive.

Neutrophils are covered with microvilli<sup>7</sup>, structures that are about 200 nm tall and form an interconnected system of ridges. Rolling of neutrophils is initiated by engagement of P-selectin glycoprotein ligand (PSGL)-1 expressed on the microvillus tip with P-selectin on the endothelium<sup>1,2</sup>. Neutrophil rolling has been studied by intravital microscopy<sup>3</sup> or *in vitro* flow chambers using trans-illumination<sup>8</sup>, DIC<sup>9</sup> or epi-fluorescence microscopy<sup>10</sup>.

Users may view, print, copy, and download text and data-mine the content in such documents, for the purposes of academic research, subject always to the full Conditions of use:[http://www.nature.com/authors/editorial\\_policies/license.html#terms](http://www.nature.com/authors/editorial_policies/license.html#terms)

Corresponding author: Klaus Ley, M.D., Head, Division of Inflammation Biology, La Jolla Institute for Allergy & Immunology, 9420 Athena Circle Drive, La Jolla, CA 92037. (858) 752-6661 (tel), (858) 752-6986 (fax), klaus@liai.org.

### AUTHOR CONTRIBUTIONS

P.S. contributed to experiment design, performed all experiments and image analysis. E.G. and A.G. designed the microfluidic device. M.K.P. performed ETMA simulations. H.Z. was involved in negative separation of mouse neutrophils from bone marrow. P.S. and K.L. wrote the manuscript. K.L. contributed to experiment design and supervised the project.

Note: Supplementary information is available on the Nature Methods website.

### COMPETING FINANCIAL INTERESTS

The authors declare no competing financial interests.

However, the “footprint” of a rolling neutrophil, which is the region of the cell membrane interacting with the P-selectin substrate, cannot be visualized by these techniques.

Recently, total internal reflection fluorescence (TIRF) microscopy has been used to map the distribution of adhesion molecules relative to the surface microtopography of stationary neutrophils<sup>11</sup>. Because TIRF microscopy penetrates only 100 to 200 nm above the cover slip, the footprint of a neutrophil and the pattern of the adhesion points can be clearly resolved. If the fluorochrome is uniformly distributed in the cell, the  $z$  positions above the cover slip can be estimated using Variable Angle-TIRF (VA-TIRF). VA-TIRF requires the cell to be stationary and therefore cannot be used for quantitative TIRF of rolling neutrophils.

Here, we introduce quantitative dynamic footprinting (qDF) microscopy which is an adaptation of TIRF microscopy and allows the estimation of  $z$  distances in the footprint of rolling neutrophils by breaking the calibration procedure into two steps. First, the distance,  $z_0$ , of the closest approach of a stationary neutrophil with the cover slip is estimated using VA-TIRF (Fig. 1a; Supplementary Fig. 1-3 and Online Methods). Then, in the qDF image of a rolling neutrophil, the pixel with maximum intensity is considered to be at  $z_0$  from the cover slip, and the  $z$  distance of the other pixels is calculated by addition of  $z_0$  to the relative separation,  $\delta$ , of each pixel from the one with maximum intensity (Fig. 1b; Eq. 9a and 9b in Supplementary Note). We used qDF microscopy to study neutrophil rolling in whole blood in a specially designed microfluidic perfusion device (Supplementary Figs. 4-7). We use cells from knock-in mice in which green fluorescent protein (GFP) is expressed in all neutrophils as a soluble cytosolic protein under the control of the endogenous lysozyme M (LysM, gene name, *Ly2*) promoter. Since GFP is distributed homogeneously in the cytosol, the fluorescence emission intensity  $I_F$  decays exponentially with  $z$  (Fig. 1b; Eq. 3a in Supplementary Note). In other experiments, we use the membrane dye DiI to label the plasma membrane (Fig. 1b; Eq. 3b in Supplementary Note).

Observation of GFP-expressing and DiI-stained neutrophils ( $n=16$ , representative examples in Figs. 2c-i) rolling on a P-selectin coated glass substrate shows that the area of closest contact ( $\sim 35$  nm above the substrate) is very small ( $\sim 0.1 \mu\text{m}^2$ ). The pattern of microvilli ridges is resolved by qDF (Fig. 2a), but not epi-fluorescence (Fig. 2b). Microvilli are preserved in the footprint where the neutrophil is in contact with the substrate (Supplementary Video 1). We quantified (Eq. 9a in Supplementary Note) the distances of different features from the glass substrate in qDF images (Figs. 3a-b) and produced 3D reconstructions of the cell surface topography in the contact zone (Figs. 3c-d) in which a microvillus was defined as a conical protrusion longer than 25 nm in  $z$ -direction. These renditions show that microvilli are at a distance of about 70 nm (equilibrium length of the P-selectin-PSGL-1 bond<sup>6,12</sup>) near the leading edge of the cell, compressed under the cell center, and extended beyond the equilibrium bond length at the rear of the cell, where they finally break away from the substrate. The closest approach is  $z_0 \sim 25$  nm, consistent with the short axis of casein, the protein used to block the sites on the glass not occupied by P-selectin. The individual microvilli were preserved over time and could be tracked in the footprints of rolling neutrophils (Figs. 3f-h). The distances between microvilli and the substrate under the footprint of the neutrophil were similar for GFP-expressing and DiI-

labeled neutrophils (Fig. 3e and Supplementary Figs. 11 and 12). The average distance at bond breakage was  $133 \pm 5$  nm (mean  $\pm$  s.e.m;  $n = 13$ ), suggesting that the maximum strain on the P-selectin-PSGL-1 bonds is  $\sim 90\%$ . The footprint at  $z = 100$  nm (Fig. 3b) was  $12 \pm 1$   $\mu\text{m}^2$  (mean  $\pm$  s.e.m;  $n = 8$ ) for a neutrophil rolling at  $6$  dyn/cm<sup>2</sup>, four times larger than the previous estimate of  $3$   $\mu\text{m}^2$  obtained using ETMA (Supplementary Fig. 13).

Above a critical force, microvilli can form tethers, when portions of the cellular plasma membrane are separated from the underlying cytoskeleton<sup>5,6,13,14</sup>. Rapidly growing tethers have been suggested to provide an optimal linkage between the cell and adhesion points (Fig. 4a), preventing excessive loading of P-selectin bonds and contributing to the ability of neutrophils to roll in a broad range of shear stress<sup>15</sup>. In all neutrophils rolling at  $6$ - $8$  dyn/cm<sup>2</sup>, we observed long tethers with anchorage points between  $1$  to  $16$   $\mu\text{m}$  behind the rear end of the contiguous footprint. Previously, tether formation has been studied by DIC microscopy<sup>9</sup>, which does not allow visualization of the tether anchorage point. Because tether anchorage points are substantially dimmer than the cell footprint in qDF micrographs (Fig. 4b), we processed the images to saturate most of the cell footprint (Supplementary Fig. 15 and Supplementary Video 2) and found the size of tether anchorage points to be near the resolution limit of light microscopy ( $\sim 0.2$   $\mu\text{m}$ ). Although tethers were observed in both GFP-expressing and DiI-labeled neutrophils, the  $z$  distances under the tether anchorage points were estimated only with DiI in the plasma membrane; this is because the estimation of  $z$  distances using cytosolic GFP requires the GFP to be distributed uniformly over a distance  $z$  greater than the wavelength of the incident laser (Eq. 3a in Supplementary Note) which is valid under the footprint ( $-4$   $\mu\text{m} < x < +4$   $\mu\text{m}$  in Figs. 3a-c;  $x$  is the distance from the cell center along the  $x$ -axis) but not under the tether anchorage points ( $x < -4$   $\mu\text{m}$  in Figs. 4b-c) which are much thinner than the wavelength of the laser. Since DiI is concentrated in the thin ( $\sim 4$  nm) plasma membrane, intensity was converted to  $z$  distance according to Eq. 9b (Supplementary Note). Tether anchorage points were found at  $125$ - $175$  nm above the substrate (Fig. 4c), consistent with major extension of P-selectin-PSGL-1 bonds (Fig. 3e). Some tether anchoring points were visibly extended along the flow direction (Supplementary Fig. 14a), encompassing areas up to  $\sim 0.73$   $\mu\text{m}^2$ . There were  $3.8$  tethers per cell on average (outside the contiguous footprint area), with the anchorage points at a mean distance of  $9.4 \pm 0.8$   $\mu\text{m}$  (mean  $\pm$  s.e.m;  $n = 31$ ) from the cell center. The large strain of the P-selectin-PSGL-1 bonds in the tether anchoring points is indicative of large forces, which suggest that tethers can make a substantial contribution to counteracting the hydrodynamic drag. However, the contribution of stressed microvilli in the footprints of rolling neutrophils cannot be ignored. They most likely share the hydrodynamic drag with long tethers. We never observed membrane (DiI) or cytosolic (GFP) material left behind (Supplementary Video 2), suggesting that tethers always completely detached from the substrate, likely due to failure of the P-selectin-PSGL-1 bonds. Occasionally, a tether-like attachment can also be seen to form in the front of the rolling neutrophil (Supplementary Video 2), which is most likely a long tether which failed to retract completely following detachment at the rear of the cell.

qDF identifies three new aspects of neutrophil rolling. First, when located under the center of the cell, the microvilli do not collapse. They remain well defined and their shape is

largely intact. Second, the footprint of a rolling neutrophil is four times larger than previously thought<sup>3</sup>. Third, all rolling neutrophils form long tethers that anchor behind the cells (well outside their footprint) via highly strained P-selectin-PSGL-1 bonds. A limitation of the current study is that neutrophils are interacting with recombinant adhesion molecules coated onto a glass substrate rather than with endothelial cells. The use of this setup is necessitated by the physics of TIRF microscopy, which requires a sharp change of the refractive index (glass vs. cell). Nevertheless, the present observations elucidate factors that can explain the ability of neutrophils to roll at wall shear stress in excess of 6 dyn/cm<sup>2</sup> *in vivo*<sup>3</sup> and in whole blood *in vitro*<sup>4</sup>.

## METHODS

Methods and any associated references are available in the online version of the paper at <http://www.nature.com/naturemethods/>.

## Supplementary Material

Refer to Web version on PubMed Central for supplementary material.

## Acknowledgments

This work was supported by WSA postdoctoral fellowship (09POST2230093) from American Heart Association (P.S.) and NIH EB 02185 (K.L.).

## References

1. Ley K, Laudanna C, Cybulsky MI, Nourshargh S. *Nat Rev Immunol.* 2007; 7:678–689. [PubMed: 17717539]
2. Hattori R, Hamilton K, Fugate R, McEver R, Sims P. *J Biol Chem.* 1989; 264:7768–7771. [PubMed: 2470733]
3. Damiano ER, Westheider J, Tozeren A, Ley K. *Circ Res.* 1996; 79:1122–1130. [PubMed: 8943950]
4. Chesnutt BC, et al. *Microcirculation.* 2006; 13:99–109. [PubMed: 16459323]
5. King MR, Heinrich V, Evans E, Hammer DA. *Biophys J.* 2005; 88:1676–1683. [PubMed: 15574709]
6. Pospieszalska MK, Ley K. *Cellular and Molecular Bioengineering.* 2009; 2:207–217. [PubMed: 20046963]
7. Finger E, Bruehl R, Bainton D, Springer T. *J Immunol.* 1996; 157:5085–5096. [PubMed: 8943418]
8. Alon R, Hammer DA, Springer TA. *Nature.* 1995; 374:539–542. [PubMed: 7535385]
9. Ramachandran V, Williams M, Yago T, Schmidtke DW, McEver RP. *Proceedings of the National Academy of Sciences USA.* 2004; 101:13519–13524.
10. Smith ML, Sperandio M, Galkina EV, Ley K. *J Leukoc Biol.* 2004; 76:985–993. [PubMed: 15075351]
11. Hocdé SA, Hyrien O, Waugh RE. *Biophys J.* 2009; 97:379–387. [PubMed: 19580776]
12. Patel K, Nollert M, McEver R. *J Cell Biol.* 1995; 131:1893–1902. [PubMed: 8557755]
13. Shao J-Y, Ting-Beall HP, Hochmuth RM. *Proceedings of the National Academy of Sciences USA.* 1998; 95:6797–6802.
14. Waugh RE, Hochmuth RM. *Biophys J.* 1987; 52:391–400. [PubMed: 3651558]
15. Park EYH, et al. *Biophys J.* 2002; 82:1835–1847. [PubMed: 11916843]
16. Tkachenko E, Gutierrez E, Ginsberg MH, Groisman A. *Lab Chip.* 2009; 9:1085–1095. [PubMed: 19350090]

17. Faust N, Varas F, Kelly LM, Heck S, Graf T. *Blood*. 2000; 96:719–726. [PubMed: 10887140]
18. Stock K, et al. *J Microsc*. 2003; 211:19–29. [PubMed: 12839547]
19. Truskey G, Burmeister J, Grapa E, Reichert W. *J Cell Sci*. 1992; 103:491–499. [PubMed: 1478950]
20. Kumosinski TF, Brown EM, Farrell HM Jr. *J Dairy Sci*. 1993; 76:931–945. [PubMed: 8486844]
21. Sachs, L. 2. Springer-Verlag; New York: 1984.
22. Pospieszalska MK, Zarbock A, Pickard JE, Ley K. *Microcirculation*. 2009; 16:115–130. [PubMed: 19023690]

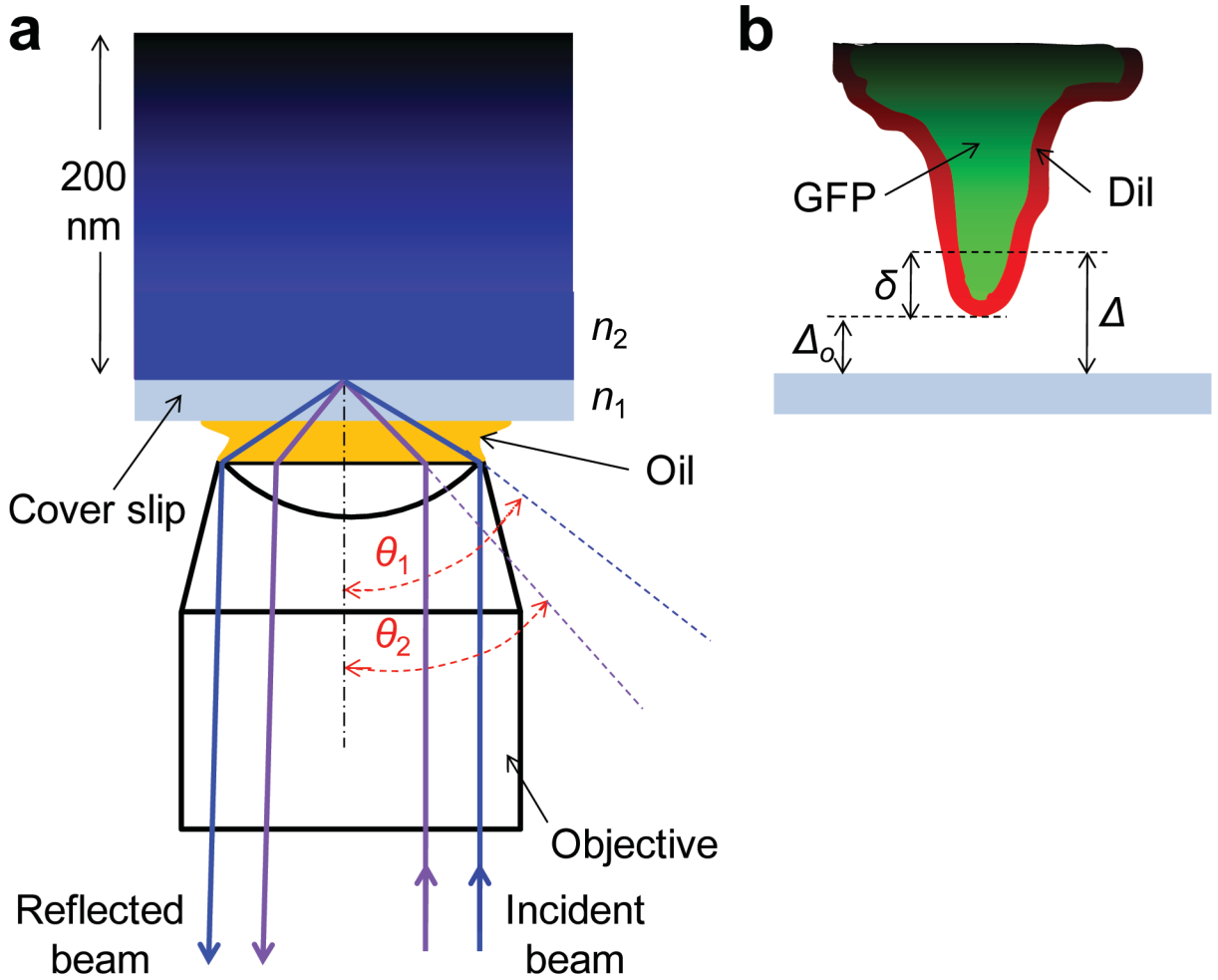


**Figure 1.**

Adaptation of TIRF for qDF microscopy. (a) In TIRF, a laser beam is incident at the glass-cell interface at an angle  $\theta_1$  or  $\theta_2$  greater than the critical angle,  $\theta_c = \sin^{-1}(n_2/n_1)$ .  $n_1$ ,  $n_2$ , refractive index of glass and cell, respectively ( $n_1 > n_2$ ). The beam undergoes total internal reflection and an evanescent wave (blue) is established on the cell side of the cover slip. (b) The evanescent wave excites GFP in the cytoplasm or DiI in the plasma membrane.  $\Delta_o$  is the distance of closest approach between the neutrophil and the cover slip.  $\Delta$  is the  $z$  position of any region in the neutrophil footprint, such that  $\Delta = \Delta_o + \delta$ .

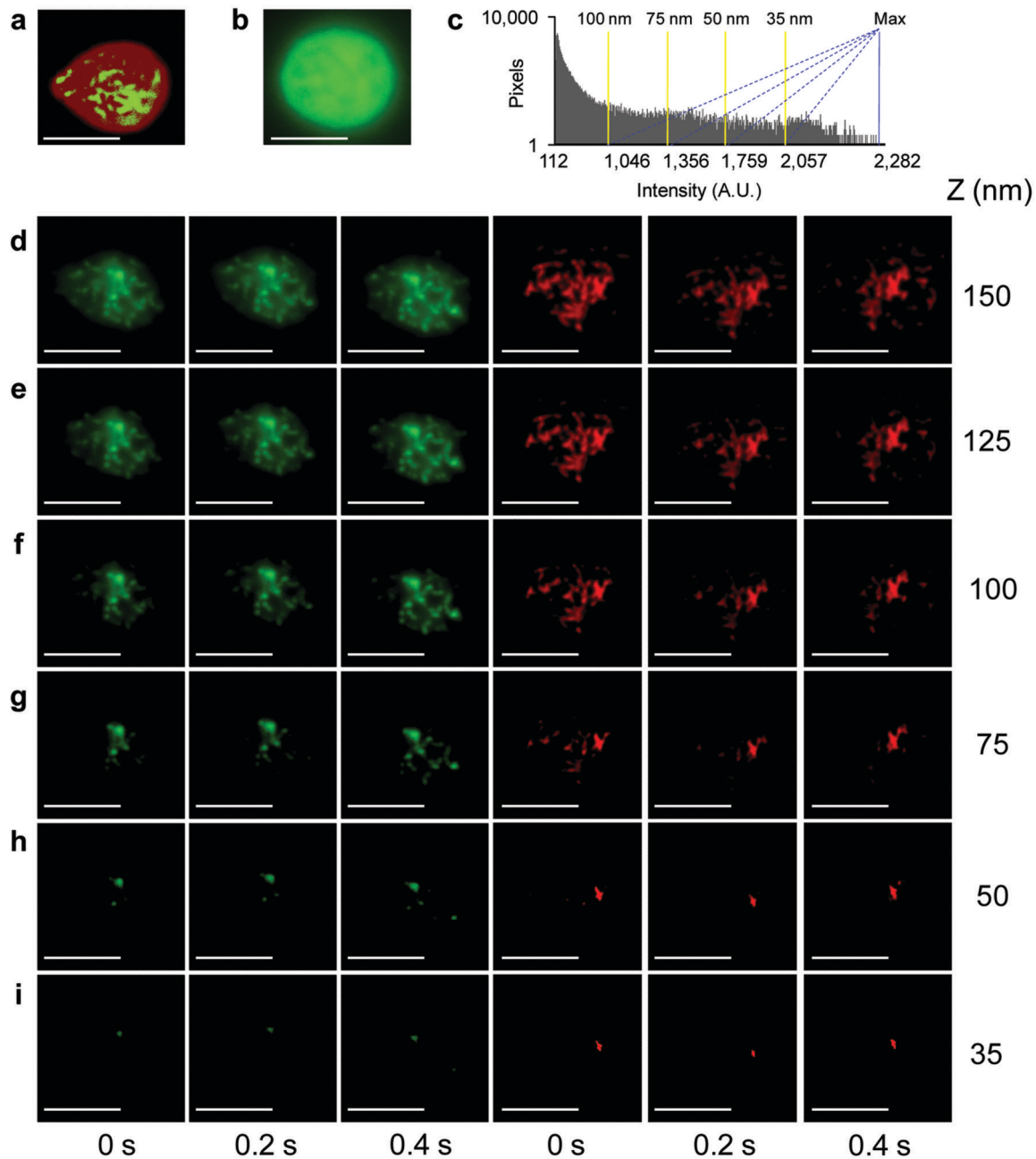


**Figure 2.** qDF microscopy resolves microvilli in rolling neutrophils. **(a, b)** Superimposed qDF (green) and bright field image (red) **(a)** and epifluorescence image **(b)** of a GFP-expressing neutrophil rolling on P-selectin. **(c)** The intensity histogram of the qDF image of a neutrophil expressing GFP thresholded to reveal footprints at different distances (as shown) from the cover slip (refer to Online Methods). Intensity histogram of a DiI-labeled neutrophil is shown in Supplementary Figure 8. **(d-i)** qDF images of a rolling GFP-expressing neutrophil (green) or a DiI-stained neutrophil (red) thresholded to exclude

features above distance  $z$  (shown on right) from the cover slip. Left to right in each row are successive images of the same cell at the indicated times. The cells are rolling from left to right. Scale bars 5  $\mu\text{m}$ . Wall shear stress 6  $\text{dyn}/\text{cm}^2$

Author Manuscript

Author Manuscript

Author Manuscript

Author Manuscript



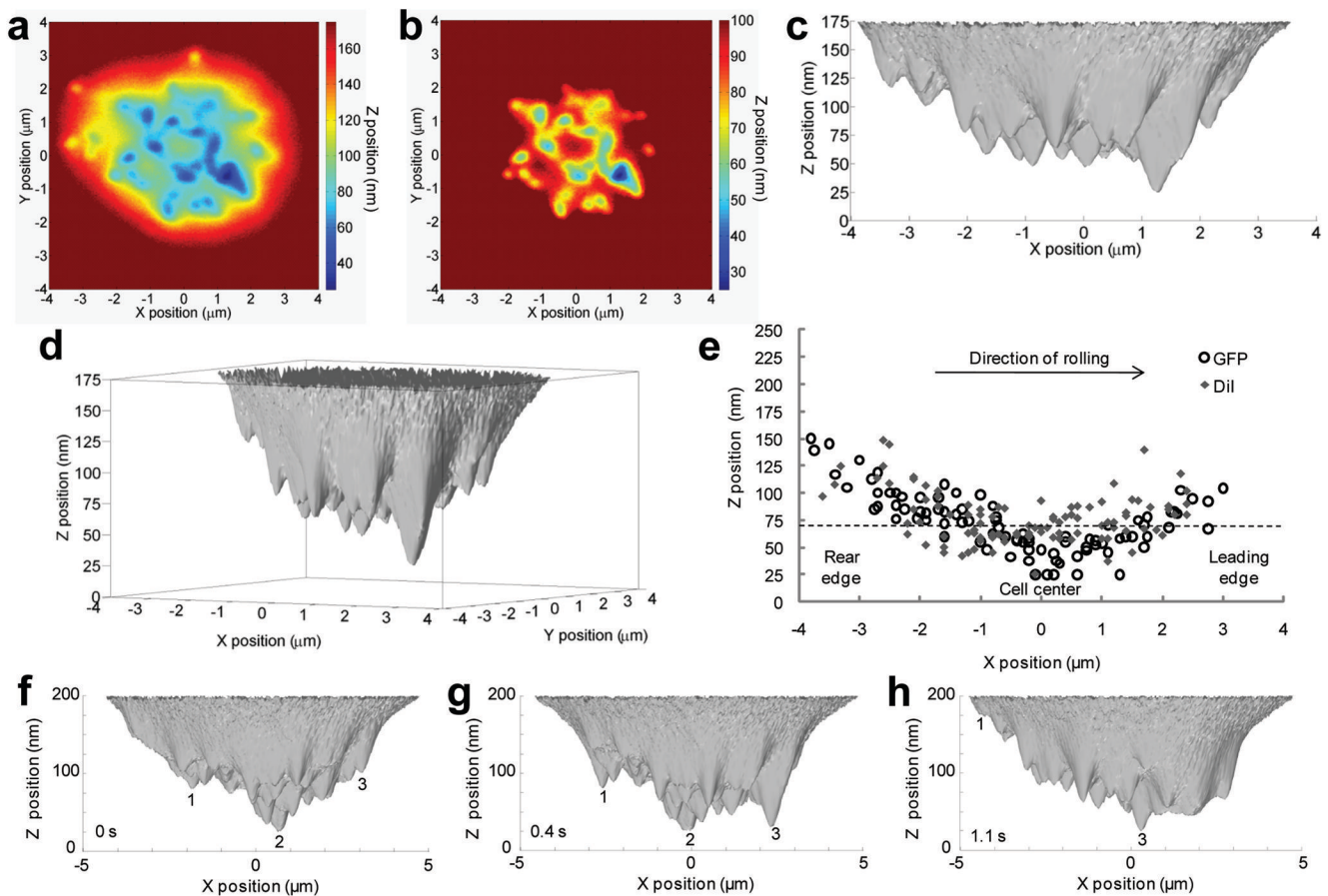


**Figure 3.**

Footprints of rolling neutrophils identify locations of stressed and compressed bonds. **(a-c)** Footprint of a rolling GFP-expressing neutrophil (flowing in  $x$ -direction) encoded as 2D color maps where regions in the footprint within 175 nm **(a)** or 100 nm **(b)** of the cover slip are encoded using the indicated color scheme. 3D surface map **(c)** show the  $x$  and  $z$  coordinates of individual microvilli tips in the footprint. Footprints of two more GFP-expressing neutrophils are shown in Supplementary Figure 9. **(d)** 3D view of panel **c**. **(e)** The  $z$  position of microvilli tips in the footprints of GFP-expressing ( $n = 5$  cells) and DiI-stained ( $n = 5$  cells) neutrophils rolling on P-selectin at  $6 \text{ dyn/cm}^2$  plotted as a function of  $x$  position from the center of the cell. Microvilli within  $1 \mu\text{m}$  on either side of the neutrophil along the  $y$ -axis are shown. The dashed line represents the unstressed length ( $\sim 70 \text{ nm}$ ) of the P-selectin-PSGL-1 bond. **(f-h)** 3D maps of a GFP-expressing neutrophil rolling on P-selectin at indicated times. Three microvilli are labeled. Microvillus 2 is on the back side of the cell at  $t = 1.1 \text{ s}$  and is therefore not visible (also see Supplementary Fig. 10). Wall shear stress  $6 \text{ dyn/cm}^2$

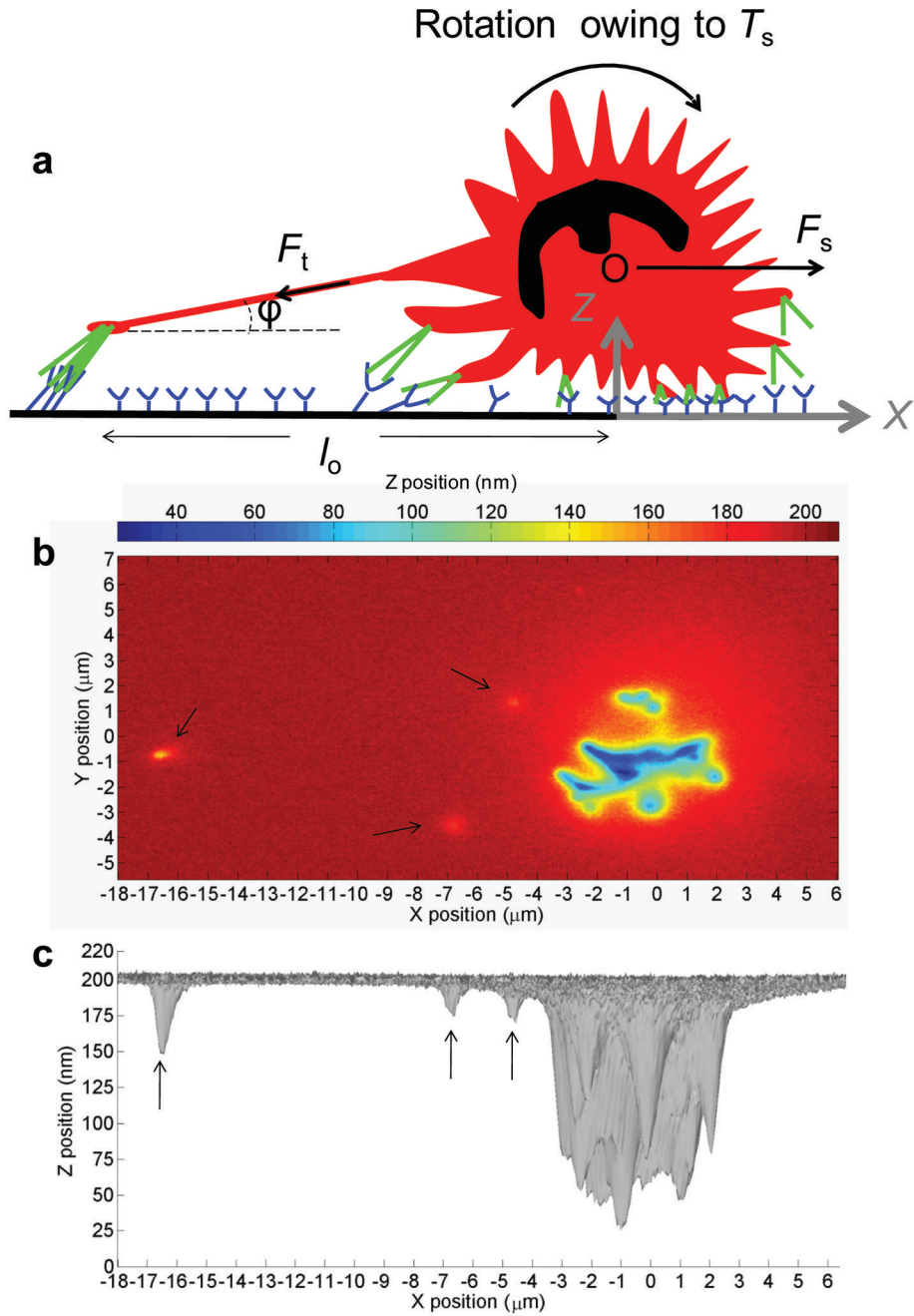


**Figure 4.** Footprints reveal anchorage points of long tethers at the rear of rolling neutrophils. **(a)** Schematic (not to scale) of a neutrophil rolling on P-selectin.  $F_s$  and  $T_s$  are the hemodynamic shear force and torque,  $F_t$  is the tether force,  $\phi$  is the tether angle,  $l_o$  is the distance of the tether anchorage point from the cell center, P-selectin on the glass substrate and PSGL-1 on the microvilli tips shown in blue and green, respectively. **(b, c)** Footprint of a rolling DiI-stained neutrophil encoded as 2D color map **(b)** and 3D surface map **(c)**. Tether

anchorage points are marked with black arrows. Footprints of two more DiI-stained neutrophils are shown in Supplementary Figure 14. Wall shear stress 8 dyn/cm<sup>2</sup>

Author Manuscript

Author Manuscript

Author Manuscript

Author Manuscript